



ARTICLE

Cloning and Function Identification of a Phytoene Desaturase Gene from *Eucommia ulmoides*

Jiali Wang¹, Xiangmei Chen¹, Xiaozhen Huang¹, Yichen Zhao^{1,*} and Degang Zhao^{1,2,*}

¹The Key Laboratory of Plant Resources Conservation and Germplasm Innovation in Mountainous Region (Ministry of Education), College of Tea Sciences, College of Life Sciences, Guizhou University, Guiyang, 550000, China

²Plant Conservation Technology Center, Guizhou Key Laboratory of Agricultural Biotechnology, Guizhou Academy of Agricultural Sciences, Guiyang, 550000, China

*Corresponding Authors: Yichen Zhao. Email: yczhao@gzu.edu.cn; Degang Zhao. Email: dgzhao@gzu.edu.cn

Received: 27 September 2022 Accepted: 28 November 2022

ABSTRACT

The phytoene desaturase (*PDS*) encodes a crucial enzyme in the carotenoid biosynthesis pathway. Silencing or inhibiting *PDS* expression leads to the appearance of mottled, chlorosis, or albino leaves. In this study, the CDS sequence of *EuPDS* (*Eucommia ulmoides* Phytoene Desaturase) was first cloned and then *PDS* was silenced in *Nicotiana benthamiana*. Result showed the expression level of *EuPDS* in leaves was higher than that in the roots and stems. In *N. benthamiana* leaves, which were treated by *Agrobacterium* for 24 h, photo-bleaching was shown on the fresh leaves one week after injection and the transcript level of *PDS* was down-regulated during the period of emersion. This suggested that *EuPDS* could silence *PDS* of *N. benthamiana*, so as to cause the phenotype of leaf whitening. *PDS* is the main reporter gene involved in virus-induced gene silencing (VIGS). This study offered molecular evidence for identifying *PDS* gene involved in Carotenoid's biosynthesis pathway and the regulation networks in *E. ulmoides*. It also laid a useful foundation for study on leaf discoloration mechanism of other woody plants.

KEYWORDS

Eucommia ulmoides; *EuPDS*; virus-induced gene silencing; TRV; relative expression

1 Introduction

Eucommia ulmoides Oliver, a medicinal edible tonic herb used in traditional chinese medicine (TCM) [1], is a single *Eucommiagenus* species of the *Eucommiaceae* family [2,3]. The results demonstrated that secondary metabolites such as lignin, naphthenes, phenylpropane, polysaccharides, flavonoids, amino acids and gutta-percha were of great importance in the pharmacological effects [4–6]. Recent pharmacological researches indicated that *E. ulmoides* has anti-aging, anti-cancer, bone cell proliferation, cardiovascular and immune control functions [7–9]. In recent years, *Agrobacterium*-mediated regenerative transformation has been successfully applied in *E. ulmoides* [10]. However, because of taking root and endophytic fungal contamination problems, it is difficult to obtain transgenic plants and to verify the gene function of *E. ulmoides*, which requires the development of genetic transformation strategies that bypass their inherent barriers.

Virus-induced gene silencing (VIGS), associated with post-transcriptional gene silencing, is a useful tool to protect plants and other organisms from infections that are naturally present [11]. Double-stranded RNA



(dsRNA), the viral vectors with unique exogenous genes, is involved in VIGS. In plants, RNA interference (RNAi) treated by dsRNA are processed by Dicer-like nuclease, the dsRNA degraded into small interfering RNA (siRNAs) ranging in length from 21 to 25 nt. These plant siRNAs reduced the corresponding targeted mRNAs genes, resulting in its degradation [11]. VIGS vectors originated from tobacco rattle virus (TRV) are widely used because of their distinct symptoms of infection, the ability to silently clone fragments and infect meristems [12].

Carotenoids are significant pigments that contribute to the variety of colors found in plant organs. The different colors of pigment match known pigments, which make up the red, green, and yellow colors of petals. Carotenoids are lipid-soluble pigments produced by photosynthetic organs, which vary in solubility depending on the species and environment [13]. Currently, the major carotenoids involved in photosynthesis are the lutein and carotene [14]. Phytoene desaturase (PDS) is the first discovered enzyme in the plant carotenoid biosynthesis pathway. *PDS* encodes a phytoene desaturase, which catalyzes a critical step in the carotenoid biosynthesis pathway, thus, recognized as an indicator for VIGS [15]. The silent phenotype of VIGS-*PDS* was utilized as a visual indicator of a VIGS efficacy in numerous plants, such as tomato [16], *Forsythia* [17] and *Nicotiana benthamiana* [18]. In the color of flowers or fruits, it has been catalyzed the synthesis colorless of colored carotenoids and, at the transcriptional level regulates the accumulation of carotenoids [19]. At the moment, *PDS* has been cloned and reported in a variety of plants, such as *SrPDS* (*Streptocarpus rexii*) [20], *SmPDS* (*Solanum melongena*) [21] and *PhPDS* (*Petunia hybrida*) [22].

Nowadays, the complete sequence of *E. ulmoides PDS* (*EuPDS*) is available in the *E. ulmoides* database [1]. However, the *EuPDS* gene has not been used till now. Therefore, the purpose of this study was to cause phenotypic function loss in order to better understand gene function and to facilitate a comparative approach. In order to obtain albinized plants and identify the biological function of *EuPDS* in tobacco plants, the research first cloned the *EuPDS*'s cDNA sequence and developed the plant viral vector pTRV2-*EuPDS*, which was injected into tobacco leaves by *Agrobacterium*-mediated infection. The findings not only establish a platform for further investigation of this gene's mechanism of color creation, but also give a reporter gene for the construction of an *E. ulmoides* VIGS system.

2 Materials and Methods

2.1 Plant Materials and Reagents

All *E. ulmoides* seeds were cultivated at the Agricultural Biotechnology Base of Guizhou University (Guizhou, China). The pTRV2-*EuPDS* constructed in our laboratory is also the repository of *A. tumefaciens* GV3101 (Guizhou, China). RNA pure Kit and RNA extraction Kit from Kangwei Century (Beijing, China), the SYBR® Select Master Mix from Novoprotein (Suzhou, China), Taq Green PCR Master Mix (2×) and T4 DNA Ligase from Thermo Fisher Scientific (Massachusetts, USA), FastDigest *Bam*HI and FastDigest *Xba*I (Massachusetts, USA), Acetone from China National Pharmaceutical Group Corporation (Beijing, China), MES from BIOBOMEI (Hefei, China), and Migic Neo Hih-Fidelity DNA from Mei5bio, and the BeyoRT™ III First Strand cDNA Synthesis Master Mix (5×) from Beyotime (Dalian, China) were obtained from the cited locations and countries.

2.2 Plant Growth Conditions

N. benthamiana and *E. ulmoides* seeds were sown on regular trays with medium: vermiculite (weight/weight, w/w; 4:1) to keep the soil wet. After two weeks, fully cotyledons of tobacco seedlings were transplanted into new pots of potting soil of the same formula.

All work containing virus-infected material was conducted in artificial climate room, at 25°C (±2.0°C). To sustain a 16-h day/8-h night cycle, additional lighting of 3000 LX intensity from metal halide lamps was recruited. The humidity level was 65%.

2.3 *EuPDS* Gene Identification

This study identified the conserved domain of *PDS* gene from the Pfam (<http://pfam.xfam.org/>) database, compared the homologous sequence with the amino acid sequence in *E. ulmoides* database, and successfully found *EuPDS* gene (ID: GWHTAAAL009905). Total RNA was obtained from *E. ulmoides* leaves with RNA extraction kit from Kangwei Century and then reversed transcribed to cDNA from Beyotime. Primers were designed based on the *PDS* sequence of *EuPDS* from *E. ulmoides* database. High-fidelity thermostable DNA polymerase was employed to produce one complete fragment. The *PDS* gene was employed in PCR using *E. ulmoides* cDNA templates to produce two overlapping fragments that were sequenced. We successfully cloned the CDS sequence of *EuPDS*. Positive clones of each fragment were identified via DNA sequencing (BGI, Beijing, China).

2.4 *VIGS* Vector Construction and Agro-Infiltration

The pTRV1 and pTRV2-*VIGS* vectors were obtained from Bio-Transduction Lab Co., Ltd. (China). This paper made use of one constructed, including pTRV2-*EuPDS*. *EuPDS* fragments up to 398 bp in length were amplified from the *Eucommia* cDNA library using M5 Magic Neo high-quality DNA polymerase. 100 ng of purified PCR product was inactivated by T4 DNA polymerase in 1× buffer containing 5 mM/L dATP at 12°C for 15 min, then at 75°C inactivate for 20 min. Meanwhile, 500 ng of linearized TRV2 (YY13) vector digested with *Xba*I was treated by dTTP for T4 DNA polymerase (Fig. S1). Transfer 2 μL of the treated TRV2 vector into 3 μL of the treated PCR product and incubate for 10 min at 70°C and 10 min at 22°C. The entire reaction solution was transformed into competent *E. coli* DH5α cells. Positive clones were determined via PCR amplification and sequencing (Fig. S2).

By the freeze-thaw procedure, the plasmid pTRV2-*EuPDS* was transformed into *Agrobacterium*, and positive colonies were found using colony PCR (Fig. S3). Amplification of the PCR product was performed using the signed verification primers (Table 1). The *Agrobacterium tumefaciens*-mediated infiltration method used was that of Burch-Smith et al. [23]. The *Agrobacterium* pTRV1 and pTRV2, as well as pTRV1 and TRV-*EuPDS*, were then mixed 1:1 and cultured at room temperature for 3 h. Leaf infiltration was used to infect the first or second pair of newly emerging leaves.

Table 1: Primers used in PCR and quantitative PCR

Usage	Genes	Nucleotide sequence (5'-3')
CDS cloning	<i>EuPDS</i>	F: ATGGCCTCTTCTTCTTTG R: TCAGACTAGAGTTAACTCGTC
Target fragment cloning	<i>EuPDS</i>	F: GAACCTGAACATTATCGGG R: GCTTTATCATAAGTCTTAAGC
TRV2:EuPDS construction	<i>EuPDS</i>	F: cgggatccGAACCTGAACATTATCGGG R: gctctagaGCTTTATCATAAGTCTTAAGC
TRV virus testing	pTRV1	F: TTACAGGTTATTTGGGCTAG R: CCGGGTTCAATTCCTTATC
	pTRV2	F: ATTTGTTTTATGTTTCAGGC R: ATGTCAATCTCGTCGTAGGTTTA
	pTRV2 1F	AGGGAGTGGGATTTCTTTGAC 1R: ATTATCCAATCCTTCAGCCCG
qRT-PCR for <i>PDS</i>	<i>β-Actin</i>	F: GATCTTGCTGGTGGTGATCT R: ACTTCCGGACATCTGAACCT
qRT-PCR for Actin	<i>PDS</i>	F: TTTGGCACTATTCCTTCG R: ATTCTCCACTGGCGTCTTC

2.5 *Virus-Induced Gene Silencing*

The *PDS* participated in chlorophyll biosynthesis was silenced in *N. benthamiana*. After a seedling grew six true leaves, the undersides of the leaves were gently rubbed with a 10 μL tip and then inoculated with *A. tumefaciens* using a 2.5 mL needleless syringe. The plant that was not silenced served as controls (infiltrated with *A. tumefaciens* of empty vectors pTRV1 and pTRV2).

2.6 Virus Detection and Quantitative Real-Time PCR (qPCR)

Plant leaves samples were collected and immediately frozen in liquid nitrogen, and total RNA was obtained from fresh leaf tissue of silenced with the RNA plant extracting Kit. First-strand cDNA was synthesized via the BeyoRT™ III First Strand cDNA Synthesis Master Mix (5×). For RT-PCR, 1 μL of first-strand cDNA was diluted. As a template in a reaction using the KAPA SYBR Quantitative PCR Kit in a Step One Plus Real-Time PCR System. The cDNA was diluted to 5 ng/μL. To determine the presence of TRV, two sets of particular primers were used to amplify pTRV1 and pTRV2 (Table 1). The qPCR was carried out in three biological replicates using the NovoProtein SYBR® Select Master Mix in 10 μL reactions. The following parameters were utilized for amplification: 95°C pre-denaturation for 3 min; 40 cycles of denaturation at 95°C for 10 s, annealing at 60°C for 10 s and extension at 72°C for 30 s.

2.7 Quantification of Pigments

Place 0.5 g of fresh uninjected tobacco leaves, no-load injection leaves, and leukized fresh leaves in a sterile treated 15 mL centrifuge tube, add 5 mL extract (80% acetone: 95% ethanol = 1:1) and soak in the dark. After two days, the leaves were almost entirely decorated, and the supernatant was collected in a cuvette. Photometric measurements were performed at 662, 645 and 470 nm [24,25].

2.8 Statistical Analysis

SPSS21.0 software was used to analyze the qRT-PCR data in all of these experiments. $p < 0.05$ is considered significant difference. Each group was repeated independently at least three times. Data analysis and sequence analysis were carried out with Excel 2007, and DNAMAN 5.0 and a public website (<https://www.ncbi.nlm.nih.gov/>) database, respectively.

3 Results

3.1 Cloning of *EuPDS* Gene in *E. ulmoides*

When *PDS* is deleted, silencing of *PDS* induce a characteristic photobleaching. The whole sequence of this gene was cloned successfully using PCR technology and re-confirmed the sequence by Sanger sequencing (Fig. 1).

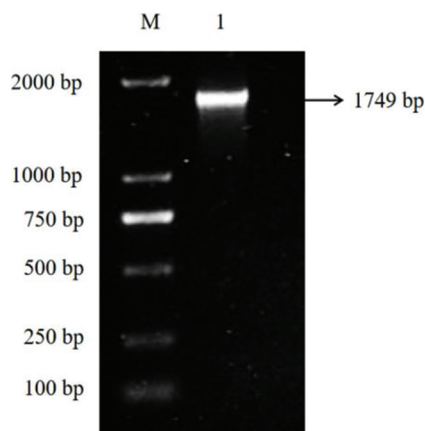


Figure 1: A full-length cDNA of *PDS* gene from *E. ulmoides* was obtained through PCR. M: DL 2000 Marker 1: PCR amplification product of *EuPDS* gene

3.2 Cloning and Bioinformatics Analysis of *EuPDS* Gene

According to the sequence information in the genome database of *E. ulmoides* constructed earlier in our laboratory, the cDNA fragment (1,749 bp) of *E. ulmoides phytoene desaturase (PDS)* gene encoding 583 amino acids was obtained by RT-PCR. The predicted molecular weight of *EuPDS* protein is

64,455.10 Da, and its theoretical isoelectric point is 8.79. The total number of negatively charged residues (Asp and Glu) is 64; the total number of positively charged residues (Arginine and Lysine) is 72. The instability index of *EuPDS* protein is 40.86, suggesting that *EuPDS* is an unstable protein. The secondary structure analysis with SOPMA indicated that putative *EuPDS* protein contained an α -helix (40.21%), an extended chain (14.78%), a random coil (40.38%), and a β -turn (4.64%). The average protein hydrophilicity value of *EuPDS* is -0.141 , which is moderately hydrophilic. The protein is predicted to contain an amino acid oxidase structure without transmembrane domain and signal peptide. The encoded protein was found to be 69.70% homologous to the *PDS* protein of *N. benthamiana*, *A. thaliana*, *Capsicum annuum*, *Bitter Gourd*, and *Populus trichocarpa* (Fig. 2). The effectiveness of silencing is based on length of a gene fragment, with the best suitable fragment lengths between 150 and 500 bp, and the minimum sequence length for gene silencing is between 21 and 25 bp. The homology of tobacco and *E. ulmoides* *PDS* genes was compared, the size of these two fragments is consistent with the size of the smallest interference fragment, so the *EuPDS* fragment with two fragments consistent with tobacco *PDS* was selected, and the fragment size was 398 bp (201 to 599 bp).

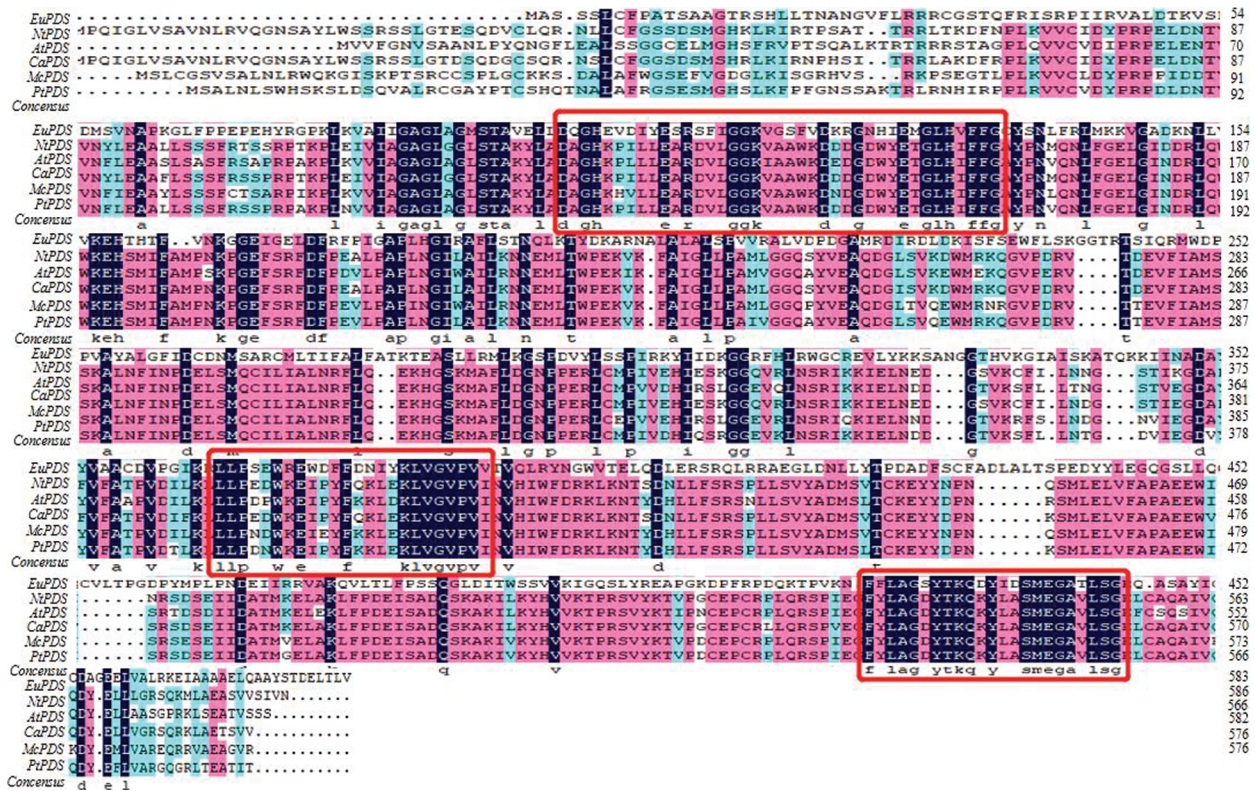


Figure 2: Homology alignment of *EuPDS* amino acid sequence. *EuPDS*: *E. ulmoides* Oliver, *GWHTAAAL009905*; *NtPDS*: *N. benthamiana*, *ABE99707.1*; *AtPDS*: *A. thaliana*, *AAA20109.1*; *CaPDS*: *C. annuum*, *CAA48195.1*; *McPDS*: *Momordica charantia*, *AAR86105.1*; *PtPDS*: *P. trichocarpa*, *XP_002321104.3*

In order to analyze the expression pattern of *EuPDS* in different tissues of *E. ulmoides*, the RNA from roots, stems and leaves was analyzed by quantitative real-time PCR technology. The result has shown that the expression level of *EuPDS* in leaves was higher than that in the roots and stems (Fig. 3).

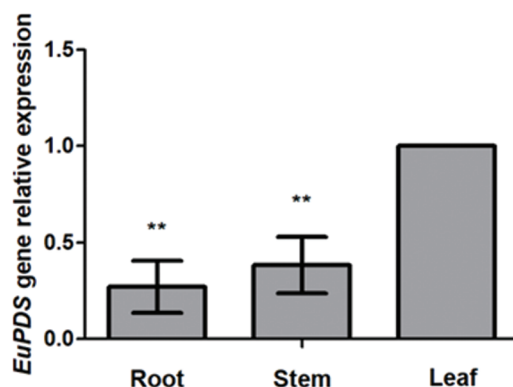


Figure 3: The expression pattern of *EuPDS* in different tissues of *E. ulomides*

3.3 Silencing of the *PDS* Gene in *N. benthamiana*

To explore whether *EuPDS* could cause *NtPDS* gene silencing in *N. benthamiana* plants, the study generated pTRV2-*EuPDS* recombinant to silence the endogenous *N. benthamiana PDS*, followed the operating approach of Martin-Hernandez et al. [14], and evaluated the gene silencing phenotypes 1 week after infiltration.

All treated plants were pruned below the infected site. Ten days later, sprouting young infected leaves harboring with the mix of pTRV1 and pTRV2-*EuPDS* exhibited total photobleaching, whereas control plants treated with the mix of pTRV2 and pTRV1 preserved their green color. New shoots and leaves of untreated plants (WT, wild-type plants), TRV2 plants (infiltrated with mixture of pTRV1 and pTRV2), silent plants with albino leaves (infiltrated with mixture of pTRV1 and pTRV2-*EuPDS*), and silent plants with new green leaves (mixed infiltration of pTRV1 and pTRV2-*EuPDS*) were collected after pruning (Fig. S4). Two strands of the virus TRV indicated the virus's presence in newly grown leaves of infected *N. benthamiana* plants (Fig. 4).

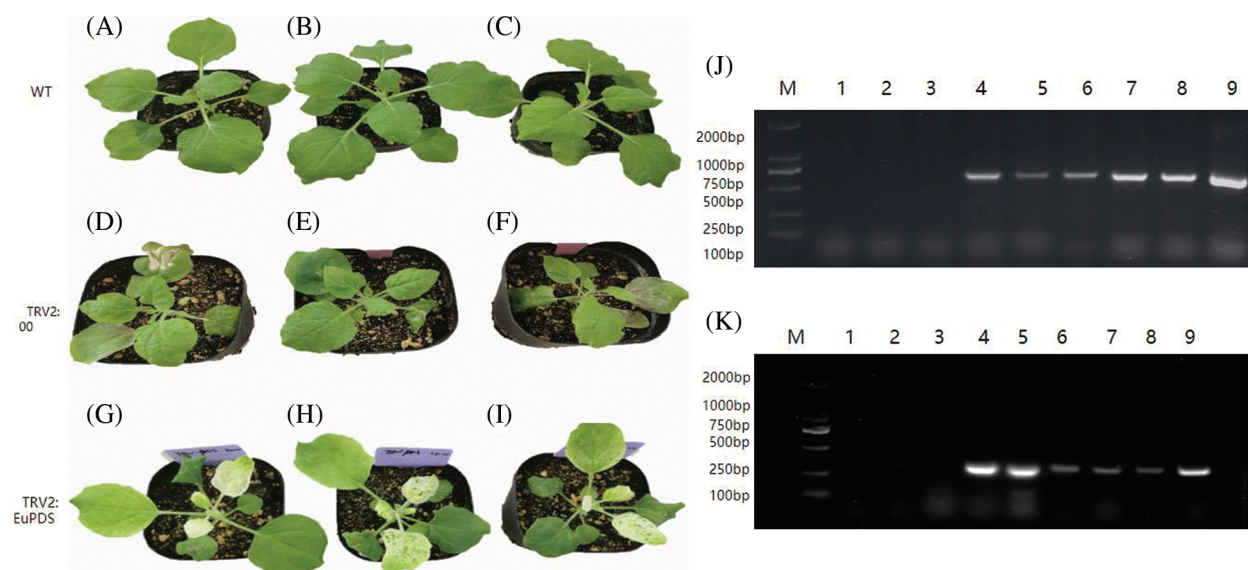


Figure 4: The detection of the two strands of viral pTRV2 and pTRV1 in *N. benthamiana* leaves. (A–C) Wild-type plants; (D–F) empty plants; (G–I) albino tobacco plants; (J) RT-PCR detection of RNA1 of TRV in tobacco, note: 1–3: wild-type plants; 4–6: empty plants; 7–9: albino tobacco plants; (K) RT-PCR detection of RNA2 of TRV in tobacco, note: 1–3: wild-type plants; 4–6: empty plants; 7–9: albino tobacco plants

1,600 *E. ulmoides* plants were injected to investigate the effects of different *Agrobacterium* concentration and different buffers on the survival rate and albino rate of *E. ulmoides* seedlings. The experimental results demonstrated that different *Agrobacterium* concentrations had different effects on the survival rate of *E. ulmoides* seedlings, and there were significant differences (Table S1). However, albino symptoms did not appear, and the RNA1 and RNA2 chains of the virus were not detected, indicating that the TRV virus could not replicate in *E. ulmoides*, so the VIGS system could not be established in *E. ulmoides* (Fig. 5). The reason may be that the *in vitro* transcription is unstable and the recombinant vector is not effectively infiltrated into the plant; it may also be related to the genetic characteristics and temperature selection of *E. ulmoides* itself. In addition, it contains a lot of *E. ulmoides* gum, the leaves are rough, and the growth is slow, which also hinders the virus from spreading in diffusion on *E. ulmoides* leaves.

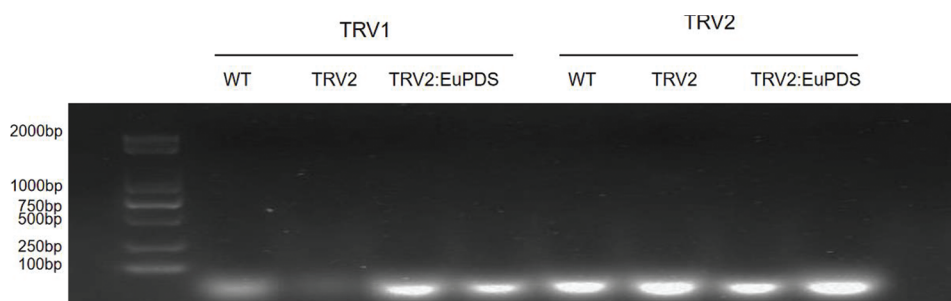


Figure 5: RT-PCR detection of RNA1 and RNA2 of TRV in *E. ulmoides*. WT: wild-type plant; TRV2: no-load control plant; TRV2: *EuPDS*: *E. ulmoides* plant injected by TRV2: *EuPDS*

3.4 Validation of the Knockdown of PDS with RT-qPCR

To verify the suppression of *PDS* in *N. Benthamiana* at the molecular level, quantitative real-time polymerase chain reaction (RT-qPCR) analysis was used. *PDS* mRNA was decreased by more than 97.6% in plants infected with pTRV2-*EuPDS* compared with controls infected with TRV alone (Fig. 6). β -actin functioned as an internal control for RNA quality for the RT-qPCR.

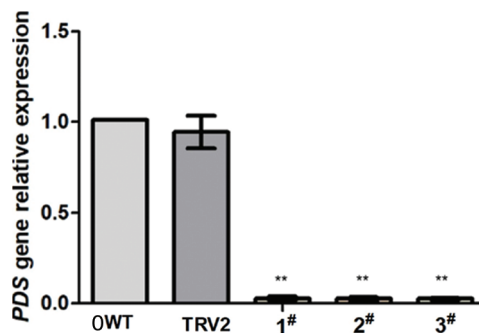


Figure 6: In the silenced plant was quantified using RT-qPCR. Error bars show standard error. WT: wild-type plant; TRV2: transfer vector plant with pTRV1 and pTRV2; 1[#], 2[#] and 3[#]: transfer vector plant with pTRV1 and pTRV2: *EuPDS* “**” indicates extremely significant level

3.5 Chlorophyll Content Measurement

Chlorophyll was obtained from green control leaves and complete photobleached leaves to verify the alterations in chlorophyll following silencing. Chlorophyll in tobacco was extracted with 95% ethanol to

determine its absorbance at 470 and 665 nm, respectively (Fig. 7). Excel2010, spass22 and GraphPad Prism were used to analyze chlorophyll a, chlorophyll b, total chlorophyll content; chlorophyll a, chlorophyll b, chlorophyll b and carotenoid content were lower than that in wild-type tobacco plants. Compared with the blank control plants (pTRV2), the contents of chlorophyll a (Fig. 7B), total chlorophyll b (Fig. 7C), chlorophyll (Fig. 7D) and carotenoids (Fig. 7E) were all obviously lower than those of the blank control plants. This shows that the change in leaf color in albino tobacco plants may be due to a change in chlorophyll concentration in response to the strength of gene expression.

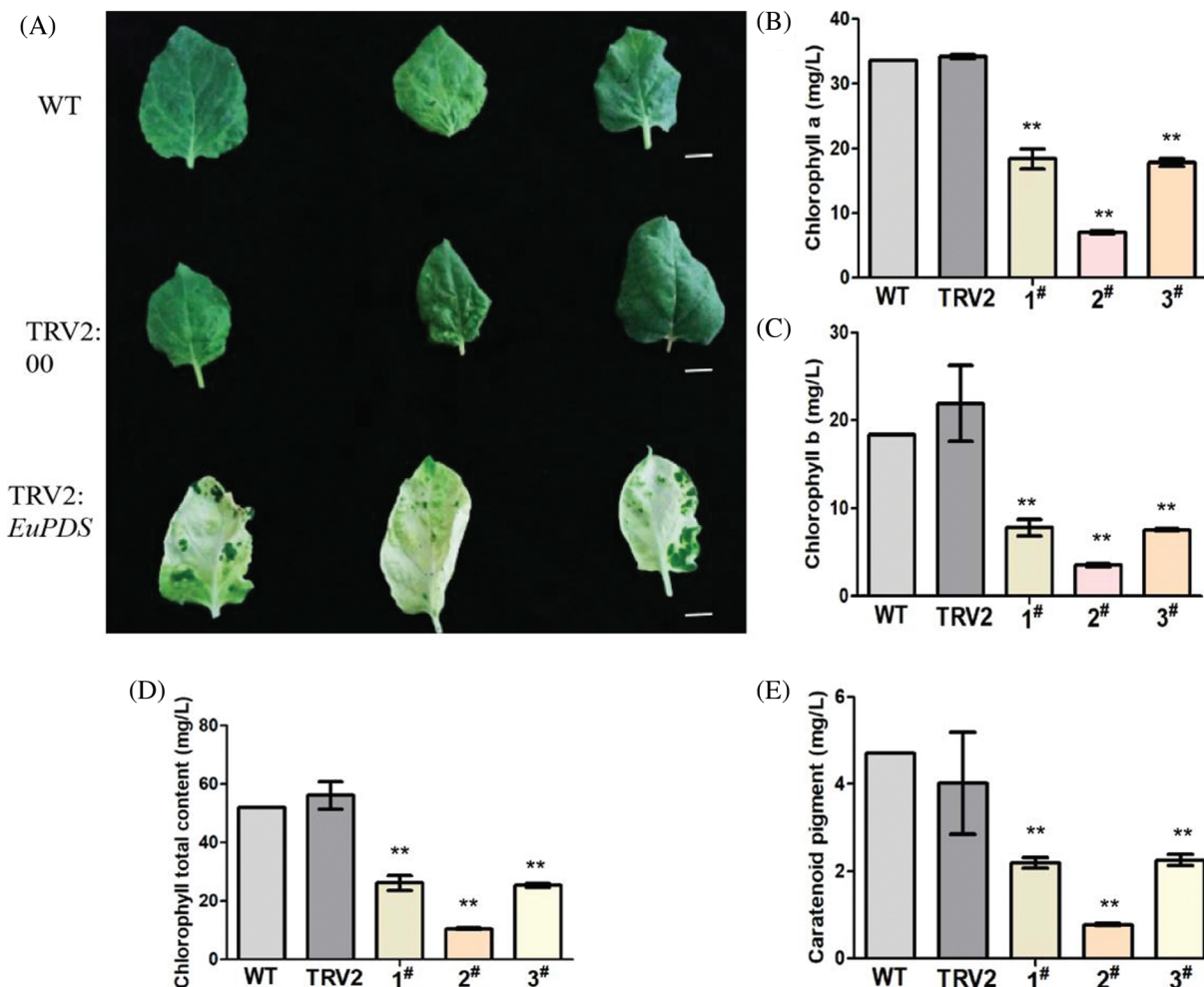


Figure 7: Chlorophyll content in leaves of albino tobacco lines. (A) Tobacco phenotypes observed. (B) The results of Chlorophyll a. (C) The results of Chlorophyll b. (D) The results of Chlorophyll total content. (E) The results of Carotenoid pigment. Notes: WT: Wild-type plants; TRV2: empty vector plants, 1#, 2# and 3#: *EuPDS* infected three albino tobacco plants; “**” indicates extremely significant level

The Cha/b ratio of each chromoprotein complex from wild-type *Arabidopsis thaliana* remained unchanged according to Hirashima et al. [26]. However, the research made by Hu demonstrated that the content of carotenoids and chlorophyll in albino leaves would be reduced by silencing *PDS* gene in *P. hybrida*, but the ratio of Cha to Chb altered [27]. In this study, similar results were obtained in Albino

tobacco plants. White tobacco plants showed a greater chlorophyll a/b ratio than CK control plants and blank control plants, as shown in Fig. 8.

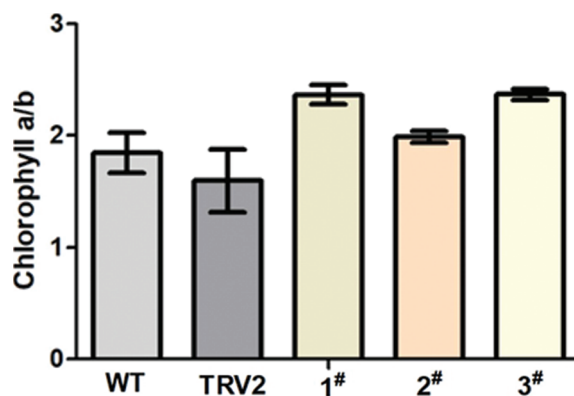


Figure 8: The ratio of chlorophyll a/b. WT: Wild-type plants; TRV2: empty vector plants, 1#, 2# and 3#: *EuPDS* infected three albino tobacco plants

4 Discussion

E. ulmoides Oliver is a commercially significant medicinal tree species that warrants further exploration considering its diverse genetic functions. In comparison to woody plants such as *Camellia oleifera* and *Populus*, the identification of the function of its genes is sluggish, and it is critical to develop a rapid, efficient, and suitable approach system for high-throughput gene function identification.

In recent years, studies on *A. thaliana* and *Vernicia fordii* have shown that *PDS* is the rate-limiting enzyme involved in carotenoid biosynthesis, which converted into colored carotenoids by introducing two double bonds into the symmetric structure of colorless phytoene substrates [28]. Plants are often able to produce phenotypes that can be visually identified after silencing the endogenous *PDS* gene or upregulating its expression. In this study, the same appearance was observed in *N. benthamiana*. Therefore, *PDS* is often used as a positive reference for gene silencing or gene editing systems, and is widely used for the regulation and construction of carotenoids biosynthesis [29].

The study cloned the whole sequence of *EuPDS* gene using PCR technology and characterized its function. The pTRV2-*EuPDS* was constructed based on TRV and injected in the leaves of *N. benthamiana*. It was shown that *PDS* is a detectable marker for VIGS in *N. benthamiana* leaves. The successful application of the VIGS of *N. benthamiana* enables us to conduct functional investigations within *E. ulmoides* rather than depending on tedious, time-consuming, and small-scale transformation. Meanwhile, *E. ulmoides* is a significant Chinese medicine with a high pharmacological value that is important in disease resistance [30]. Thus, this research provides a reporter gene for the developing VIGS technology of *E. ulmoides*, which will provide help for further study on *E. ulmoides* gene function. The successful identification of these genes will provide the basis for the yield improvement of *E. ulmoides* rubber.

5 Conclusions

This research first cloned *EuPDS* gene and identified its function. The expression pattern of *EuPDS* in different tissues of *E. ulmoides* has shown that the expression level of *EuPDS* in leaves was higher than that in roots and stems. This study constructed an efficient TRV vector using this gene. This method successfully induced a photobleaching phenotype in newly grown leaves of *N. benthamiana*. The sprouting fresh tobacco leaves showed strong photobleaching. Photometric measurements indicated that the contents of chlorophyll

a, chlorophyll b, total chlorophyll and carotenoids were all obviously lower than those of the blank control plants, but the ratio of Cha to Chb altered. This result not only provides a platform for further study of the gene's color-forming mechanism, but also provides a reporter gene for the construction of *E. ulmoides* VIGS systems.

Funding Statement: This study was funded by the National Natural Science Foundation of China (Nos. 31870285, 31660076 & 32160384), the Open Fund for Key Laboratory of Ministry of Education and Science (No. KY [2022]366), and Guizhou Province High-Level Innovative Talent Training Program Project (No. [2016]4003).

Author Contributions: ZDG, ZYC and HXZ planned and conducted the experiments. WJL and CXM implemented the experiments. WJL wrote the manuscript. All authors reviewed and approved the manuscript.

Conflicts of Interest: The authors declare that there are no conflicts of interest in this study.

References

1. He, X. R., Wang, J. H., Li, M. X., Hao, D. J., Yang, Y. et al. (2014). *Eucommia ulmoides* Oliv.: Ethnopharmacology, phytochemistry and pharmacology of an important traditional Chinese medicine. *Journal of Ethnopharmacology*, 151(1), 78–92.
2. Wu, J. M., Chen, H. X., Li, H., Tang, Y., Yang, L. et al. (2016). Antidepressant potential of chlorogenic acid-enriched extract from *Eucommia ulmoides* Oliver bark with neuron protection and promotion of serotonin release through enhancing synapsin I expression. *Molecules*, 21(3), 260.
3. Zhu, M. Q., Sun, R. C. (2018). *Eucommia ulmoides* Oliver: A potential feedstock for bioactive products. *Journal of Agricultural and Food Chemistry*, 66(22), 5433–5438.
4. Hao, S., Xiao, Y., Lin, Y., Mo, Z. T., Chen, Y. et al. (2016). Chlorogenic acid-enriched extract from *Eucommia ulmoides* leaves inhibits hepatic lipid accumulation through regulation of cholesterol metabolism in HepG2 cells. *Pharmaceutical Biology*, 54(2), 251–259.
5. Takamura, C., Hirata, T., Ueda, T., Ono, M., Migashita, H. et al. (2006). Iridoids from the green leaves of *Eucommia ulmoides*. *Journal of Natural Products*, 70(8), 1312–1316.
6. Wang, W. C., Yang, G. Q., Deng, X., Shao, F. Q., Li, Y. Q. et al. (2020). Molecular sex identification in the hardy rubber tree (*Eucommia ulmoides* Oliver) via ddRAD markers. *International Journal of Genomics*, 10, 2420976.
7. Hirata, T., Kobayashi, T., Wada, A., Ueda, A., Fujikawa, T. et al. (2011). Anti-obesity compounds in green leaves of *Eucommia ulmoides*. *Bioorganic & Medicinal Chemistry Letters*, 21(6), 1786–1791.
8. Ho, J. N., Lee, Y. H., Park, J. S., Jun, W. J., Kim, H. K. et al. (2005). Protective effects of aucubin isolated from *Eucommia ulmoides* against UVB-induced oxidative stress in human skin fibroblasts. *Biological & Pharmaceutical Bulletin*, 28(7), 1244–1248.
9. Zhang, N. D., Han, T., Huang, B. K., Rahman, K., Jiang, Y. P. et al. (2016). Traditional Chinese medicine formulas for the treatment of osteoporosis: Implication for antiosteoporotic drug discovery. *Journal of Ethnopharmacology*, 189, 61–80.
10. Feng, Y. Z., Zhang, L., Cao, H. P., Tan, X. F., Li, F. D. (2015). Transcriptome sequencing reveals fatty acid synthesis pathway in *Eucommia ulmoides* Oliv. *Hortscience*, 50(9), 371–372.
11. Bone, R. A., Landnum, J. T., Fernandez, L., Tesis, S. L. (1988). Analysis of the macular pigment by HPLC: Retinal distribution and age study. *Investigative Ophthalmology Visual Science*, 29(6), 843–849.
12. Fleischmann, P., Watanabe, N., Peter, W. (2003). Enzymatic carotenoid cleavage in star fruit (*Averrhoa carambola*). *Phytochemistry*, 63(2), 131–137.
13. Robertson, D. (2004). VIGS vectors for gene silencing: Many targets, many tools. *Annual Review of Plant Biology*, 55, 495–519.

14. Martin-Hernandez, A. M., Baulcombe, D. C. (2008). Tobacco rattle virus 16-kilodalton protein encodes a suppressor of RNA silencing that allows transient viral entry in meristems. *Journal of Virology*, 82(8), 4064–4071.
15. Cunningham, F. X., Gantt, E. (1998). Genes and enzymes of carotenoid biosynthesis in plants. *Plant Physiology*, 49, 557–583.
16. Liu, Y., Schiff, M., Dinesh-Kumar, S. P. (2002). Virus-induced gene silencing in tomato. *Plant*, 31(6), 777–786.
17. Shen, J. H., Si, W. J., Wu, Y. T., Xu, Y., Wang, J. et al. (2021). Establishment and verification of an efficient virus-induced gene silencing system in *Forsythia*. *Horizontal Plant Journal*, 7(1), 81–88.
18. Ratcliff, F., Martin-Hernandez, A. M., Baulcombe, D. C. (2001). Tobacco rattle virus as a vector for analysis of gene function by silencing. *Plant Journal*, 25, 237–245.
19. Chamovitz, D., Sandmann, G., Hirschberg, J. (1993). Molecular and biochemical characterization of herbicide-resistant mutants of cyanobacteria reveals that phytoene desaturation is a rate-limiting step in carotenoid biosynthesis. *Journal of Biological Chemistry*, 268(23), 17348–17353.
20. Nishii, K., Fei, Y., Hudson, A., Moller, M., Molnar, A. (2020). Virus-induced gene silencing in *Streptocarpus rexii* (Gesneriaceae). *Molecular Biotechnology*, 62(6–7), 317–325.
21. Liu, P. F., Wang, A. L., Du, Q. X., Du, H. Y. (2020). Chemotype classification and biomarker screening of male *Eucommia ulmoides* Oliv. flower core collections using UPLC-QTOF/MS-based non-targeted metabolomics. *PeerJ*, 8, e9786.
22. Zhou, Y. J., Deng, Y. T., Liu, D., Wang, H. Z., Zhang, X. et al. (2021). Promoting virus-induced gene silencing of pepper genes by a heterologous viral silencing suppressor. *Plant Biotechnology Journal*, 19(12), 2398–2400.
23. Burch-Smith, T. M., Anderson, J. C., Martin, G. B., Dinesh-Kumar, S. P. (2014). Applications and advantages of virus-induced gene silencing for gene function studies in plants. *The Plant Journal: For Cell and Molecular Biology*, 39(5), 734–746.
24. Yan, J., Xiang, F., Yang, P., Li, X., Zhao, X. (2021). Overexpression of *BnGA2ox2*, a rapeseed gibberellin 2-oxidase, cause dwarfism and increased chlorophyll and anthocyanin accumulation in *Arabidopsis* and rapeseed. *Plant Growth Regulation*, 93(1), 1–13.
25. Yang, P., Li, Y. X., He, C. S., Yang, J. D., Zhang, W. et al. (2020). Phenotype and TMT-based quantitative proteomics analysis of *Brassica napus* reveals new insight into chlorophyll synthesis and chloroplast structure. *Journal of Proteomics*, 214(C), 103621.
26. Hirashima, M., Satoh, S., Tanaka, R., Tanaka, A. (2006). Pigment shuffling in antenna systems achieved by expressing prokaryotic chlorophyllide a oxygenase in *Arabidopsis*. *The Journal of Biological Chemistry*, 281(22), 15385–15893.
27. Hu, L. (2017). *Effects of silent PhPDS gene on growth and development of Petunia hybrida*. Huazhong Agricultural University, China.
28. Bramley, P. M. (2002). Regulation of carotenoid formation during tomato fruit ripening and development. *Journal of Experimental Botany*, 53(377), 2107–2113.
29. Gemmecker, S., Schaub, P., Koschmieder, J., Brauseman, A., Drepper, F. et al. (2015). Phytoene desaturase from *Oryza sativa*: Oligomeric assembly, membrane association and preliminary 3D-analysis. *PLoS One*, 10(7), e0131717.
30. Fang, C., Chen, L. Y., He, M. Z., Luo, Y. Y., Zhou, M. J. et al. (2019). Molecular mechanistic insight into the anti-hyperuricemic effect of *Eucommia ulmoides* in mice and rats. *Pharmaceutical Biology*, 57(1), 112–119.

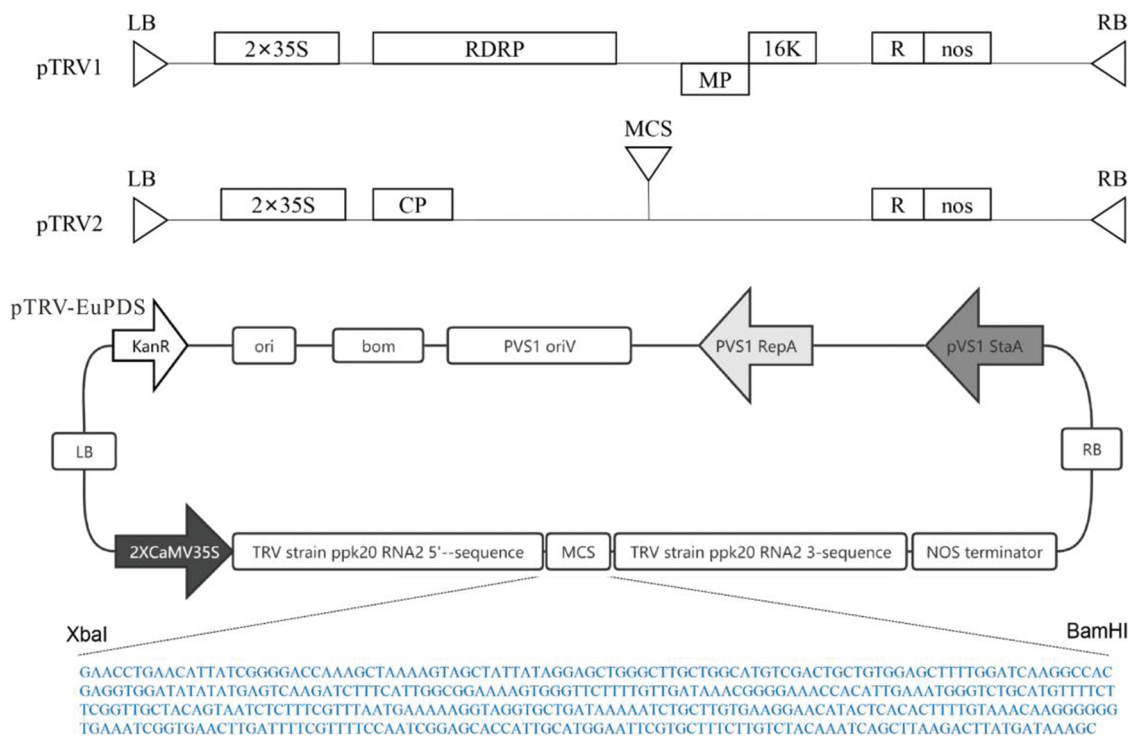


Figure S1: Schematic representation of the pTRV2-EuPDS vector

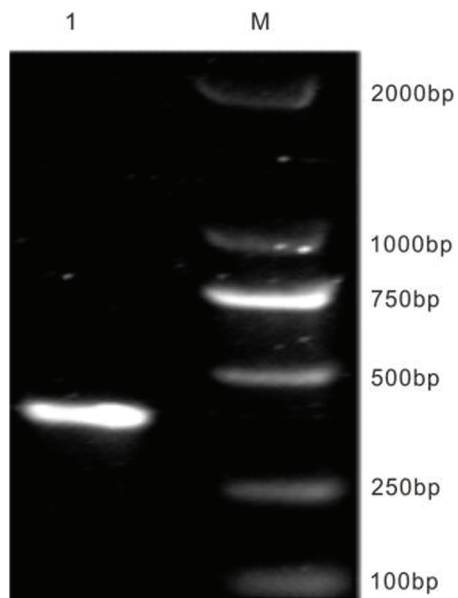


Figure S2: The amplification of *EuPDS* gene special segment. M: DNA marker DL 2000; 1: *EuPDS* special segment

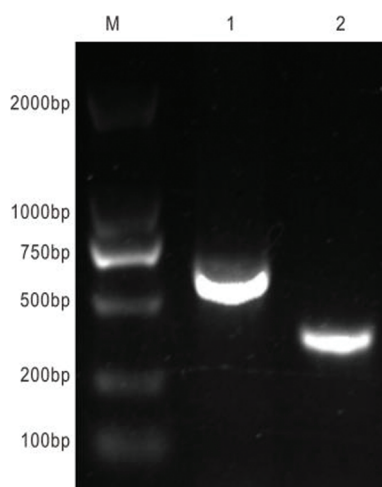


Figure S3: Results of construction of plant interference vector. M: DNA marker DL 2000; 1: Amplification segment of RNA2 premier; 2: *EuPDS* special segment

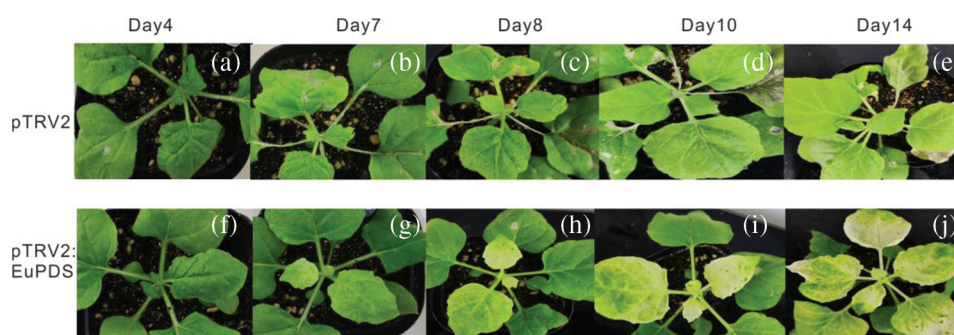


Figure S4: VIGS of *N. benthamiana* phytoene desaturase ortholog *PDS* results in varying degrees of leaf photobleaching. Note: a/f: The sprouted young leaves of 4 days after injection; b/g: The sprouted young leaves of 7 days after injection; c/h: The sprouted young leaves of 8 days after injection; d/i: The sprouted young leaves of 10 days after injection; e/j: The sprouted young leaves of 14 days after injection

Table S1: Results of *E. ulmoides* plants treated with different buffer and *A.* concentrations

The contents of buffer solution	OD ₆₀₀	Injected <i>E. ulmoides</i> plants	Survival rate	Albino rate
10 mM MES + 10 mM MgCl ₂ + 200 μM AS	0.5	200	90	0
	1.0	200	87	0
	1.5	200	88	0
	2.0	200	80	0
10 mM MES + 10 mM MgCl ₂ + 200 μM AS + 400 mg/L Cysteine + 5 mL/L Tween20	0.5	200	94	0
	1.0	200	86	0
	1.5	200	88	0
	2.0	200	82	0